ARCHIWUM ENERGETYKI tom **XLII**(2012), nr 2, 59–71

Janusz Kotowicz*
Adrian Balicki

Silesian University of Technology
Institute of Power Engineering and Turbomachinery
Gliwice

Analysis of the efficiency of the unit based on circulating fluidized bed boiler integrated with three-end high-temperature membrane for air separation

In this paper boiler with circulating fluidized bed was analyzed. For the combustion of lignite in the boiler oxygen produced in the three-end high-temperature membrane was used. Paper shows a method of determining the surface of the membranes and energy consumption of the air separation process. Boiler thermal efficiency, energy consumption of the process and air separation membrane module surface was determined as a function of oxygen recovery in the membrane. Nitrogen from the air separation unit was proposed to be used for drying lignite. For this variant characteristics of the system were determined. It was found that the thermal efficiency of the boiler in case where nitrogen was used for lignite drying increased from 76% to 87% with increasing value of oxygen recovery ratio from 0.45 to 0.9 and is higher, respectively, from 12% to 6% in comparison to the system without drying. In the proposed air separation unit required membrane surface is in the range 76500–95000 m^2.

Nomenclature

A	–	membrane surface, m^2
c	–	specific heat capacity, J/(kg K)
I	–	physical enthalpy, W
j_{O2}	–	individual oxygen flow, l/(h m^2)
L	–	membrane length, m
p_{O2}	–	oxygen pressure, Pa
Q	–	heat flux, W
r	–	enthalpy of vaporization, J/kg

*Corresponding Author. E-mail: Janusz.Kotowicz@polsl.pl

R – oxygen recovery ratio
T – temperature, K
w – moisture content in lignite
W – lower heating value, J/kg
X_{O2} – oxygen content
β – pressure ratio
η_{tk} – boiler thermal efficiency

Subscripts

a – air
c – lignite
C – air compressor
el – electric
F – feed
g – gross
n – nitrogen
P – permeate
R – retentate
s – steam
TG – gas turbine expander
vap – evaporation
VP – vacuum pump

1 Introduction

This paper presents a thermodynamic analysis of the system in which the oxygen is produced in the air separation unit based on a three-end high-temperature membrane. The system is composed of: supercritical circulating fluidized bed (CFB) boiler working in oxy-combustion technology, steam cycle, air separation unit (ASU) installation based on a three-end high-temperature membrane and the installation of fuel drying. The boiler is fed with lignite, a steam cycle is supplied by a live steam of parameters 600 °C/29 MPa and a reheated steam with parameters of 620 °C/5 MPa. Gross output of the steam generator with assumed constant steam parameters are equal to 600 MW [1,2]. The main objective of the study was to analyze the influence of drying fuel on CFB boiler thermal efficiency, as well as to investigate the permeability of the membrane module and the surface of the membrane with assumed physical parameters.

2 Method of membrane air separation

In three-end type high-temperature membranes stream of gas permeating through the membrane surface does not connect directly to another stream. Membrane is supplied with air stream but through the membrane surface permeates only oxygen. Driving force of the oxygen permeation through the membrane process is the difference of the partial pressure of oxygen in the feed and permeate streams. The pressure difference is generated by the air compressor located on the feed stream and a vacuum pump located on the permeate stream [3,4,5]. Scheme of the three-end type high temperature membrane is shown in Fig. 1.

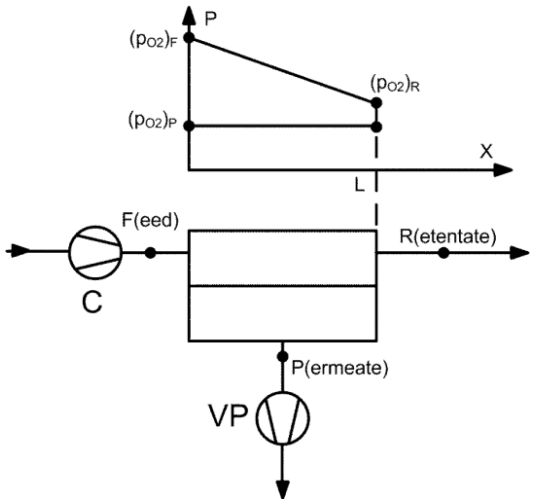

Figure 1. Three-end type high temperature membrane.

In a simple form the dependence on the amount of oxygen which has penetrated through the membrane can be represented as follows:

$$j_{O2} = C_1 \ln(\frac{(p_{O2})_F}{(p_{O2})_P}) \, . \tag{1}$$

Let us define the oxygen recovery ratio in the membrane (how much of the oxygen supplied to the membrane penetrates through the surface) by

$$R = \frac{(\dot{n}_{O2})_P}{(\dot{n}_{O2})_F} \, . \tag{2}$$

Then, the oxygen content in the retentate due to the balance of oxygen is

$$(X_{O2})_R = \frac{(X_{O2})_F(1-R)}{1-R(X_{O2})_F} \, . \tag{3}$$

If we assume a linear distribution of oxygen partial pressure along the length of the membrane on the feed side (Fig. 1) and defining a pressure ratio of the air compressor and vacuum pump as

$$\beta_C = \frac{p_F}{p_O}, \quad \beta_{VP} = \frac{p_O}{p_P}, \tag{4}$$

so from Eq. (1) we get

$$j_{O2} = C_1 \ln \beta_C \beta_{VP} (X_{O2})_F \left\{ 1 - \frac{x}{L} \frac{R \cdot [1 - (X_{O2})_F]}{1 - R \cdot (X_{O2})_F} \right\}. \tag{5}$$

The condition for the flow of oxygen through the membrane surface is that the expression under the logarithm in Eq. (5) was higher than 1. Hence, we can find limit of the oxygen recovery ratio for the assumed pressure ratios in air compressor and vacuum pump:

$$R_{lim} = \frac{\beta_C \beta_{VP} (X_{O2})_F - 1}{(\beta_C \beta_{VP} - 1)(X_{O2})_F}. \tag{6}$$

The total stream of oxygen permeating through the membrane is

$$(\dot{n}_{O2})_P = \int j_{O2} dA. \tag{7}$$

If we assume that the membrane is in the shape of a cylinder of length L and area A then

$$(\dot{n}_{O2})_P = \frac{A}{L} \int j_{O2} dX. \tag{8}$$

From (8) using Eq. (5) and after integration we obtain the formula for the surface of the membrane

$$A = \frac{m_{O2} C_1}{\ln \beta_C + \ln \beta_{VP} + \ln \frac{(X_{O_2})_F}{e} + \frac{1-R}{R(1-(X_{O_2})_F)} \ln \frac{1-R(X_{O_2})_F}{1-R}} \tag{9}$$

It was assumed that for the calculations ceramic membrane with parameters which are presented in Tab. 1 will be used. Calculations were performed for three different values of oxygen recovery ratio in the membrane: 50%, 70% and 88.55%. The stream of oxygen supplied to the combustion chamber for different oxygen recovery ratio is equal to: 139.4 kg/s, 131.7 kg/s and 128.1 kg/s, respectively. Other important assumptions for the calculations are shown in Tab. 2 [4].

For the membrane calculations aiming to determine the individual stream of oxygen permeating through the membrane surface at various points along its

Table 1. Main parameters of chosen membrane.

Parametr		Membrane A
Membrane thickness	μ	47.3
Ionic conductivity	S/m	92

Table 2. Main Assumption for the calculations.

Calculation assumptions		Membrane A
Pressure ratio in air compressor	–	13.8
Pressure ratio in vacuum pum	–	2.45
Oxygen content in feed strea	%	21
Oxygen content in permeat stream	%	10
Membrane operating temperature	K	1123.1
Feed pressur	kPa	1400
Premeate pressur	kPa	42.5

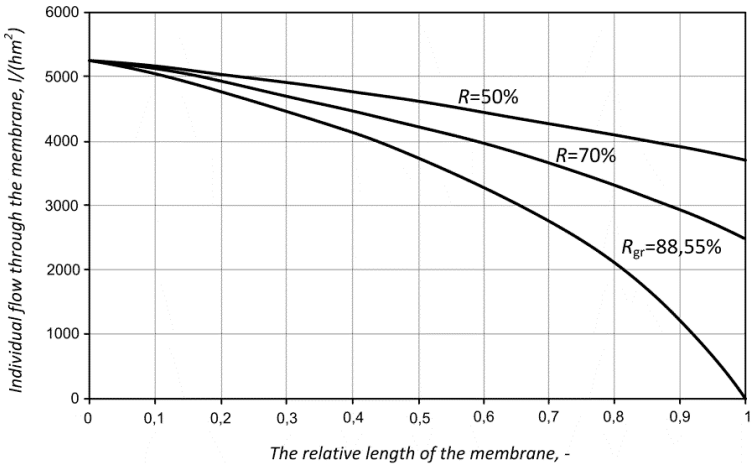

Figure 2. Individual stream of oxygen as a function of relative length of the membrane.

whole length were made. The results of this analysis are presented in Fig. 2. As it can be seen together with movement of the feed stream along the membrane, the stream of oxygen permeating through its surface decreases due to the decrease of oxygen partial pressure difference on both sides of the membrane. It was observed that with higher oxygen recovery ratio in the membrane unit significantly decreases the oxygen stream permeating through the membrane.

The second stage of the calculations was to determine the area of the membrane module. A characteristic of changes in the surface of the membrane module as a function of the oxygen recovery ratio in the membrane is shown in Fig. 3. As with the increase of the surface also increase the investment cost we should be

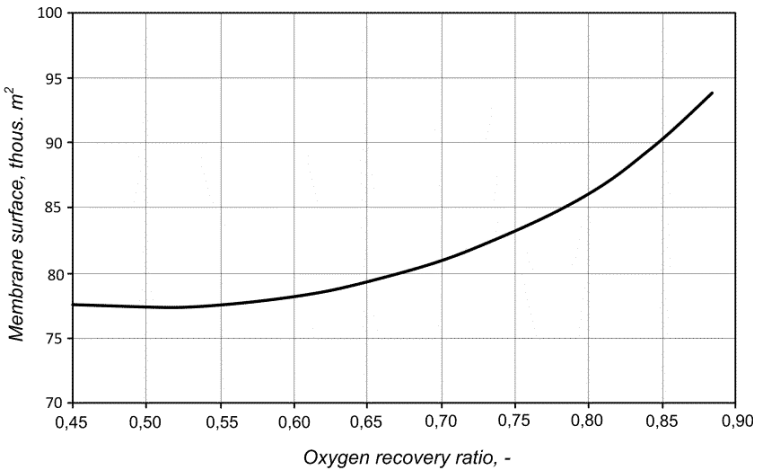

Figure 3. Membrane module surface as a function of oxygen recovery ratio in the membrane.

pursued for use in the construction of a membrane module materials that allows for maximum reduction of its surface. As it can be seen, with increasing oxygen recovery ratio in the membrane (and hence also decrease in oxygen stream permeating through the membrane surface) also increases the surface membrane module.

3 Circulating fluidized bed boiler integrated with membrane-based air separation unit

A model of a supercritical boiler with circulating fluidized bed working in oxy-combustion technology was built using commercially available computer program GateCycle and in-house codes [1,2,6,7]. In Fig. 4 a scheme of plant with CFB oxy-type boiler, air separation unit (ASU) and steam cycle is shown in a simplified way. At the stage of adopting assumption for its construction it was decided to use the fluidized bed boiler block, provided by the GateCycle software which consists of furnace chamber (AC), evaporator (EVAP) and last sections of the live steam superheater (SH II) and reheated steam superheater (RH II). In the

direction of flue gas flow this block ends with particle separator (cyclone). Behind the cyclone gas/gas type heat exchanger (PPO), in which air from ASU installation is heated to the temperature of 850 °C, was placed. Subsequently following exchangers were placed: live steam superheater (SH I), reheated steam superheater (RH I), economizer (ECO), recirculated exhaust gas heater (PRS) and nitrogen heater (NH). The last devices in the direction of flue gas flow are: electrostatic precipitator (EF), flue gas fan (W1) and the flue gas dryer (FGD). In next stage of work exhaust stream will be further directed to CCS installation [8,9,10].

It was assumed that the gross power of the steam cycle generator is fixed at 600 MW. Simultaneously, it was assumed that the steam parameters (both live and reheated), as well as feedwater stream are maintained constant. For these assumptions feedwater stream and reheated steam stream were calculated. Main assumptions for the CFB boiler are show in Tab. 3 [1,2,7]. The boiler is supplied

Table 3. Main assumptions for CFB boiler.

Lignite lower heating value	kJ/kg	9960
Feedwater flow	kg/s	43102
Feedwater temperature	°C	297
Feedwater temperature at the outlet of ECO II	°C	340
Steam temperature at the outlet of the evaporator	°C	480
Live steam temperature at the outlet of the boiler	°C	6049
Live steam pressure at the outlet of the boiler	MPa	301
Reheated steam flow at the outlet of the boiler	kg/s	36482
Reheated steam temperature at the outlet of the boiler	°C	6224
Reheated steam pressure at the outlet of the boiler	MPa	512
Temperature difference at the cold side of ECO I	K	55
Oxidant excess ratio		12
Oxygen content in oxidizer fed to the boiler	%	30
Temperature difference at the hot end of recirculated flue gas heater PRS	K	30
Ambient pressure	kPa	10132
Ambient temperature	°C	15

with lignite composed of: carbon – 28.60%, sulfur – 0.95%, nitrogen – 0.25%, hydrogen – 2.20%, oxygen – 8.00%, ash – 17.50%, moisture – 42.5%.

In the present model a three-end type high temperature membrane was treated as a black box, where at a given composition of the permeate (in this case 100% composed of oxygen) the recovery ratio of oxygen was a decision variable [4]. Recovery ratio of oxygen during the calculation was changed from the value of 45% to 90%. Heat losses were not included, so each of the streams within the membrane has a temperature of 850 °C. The pressure losses within the same

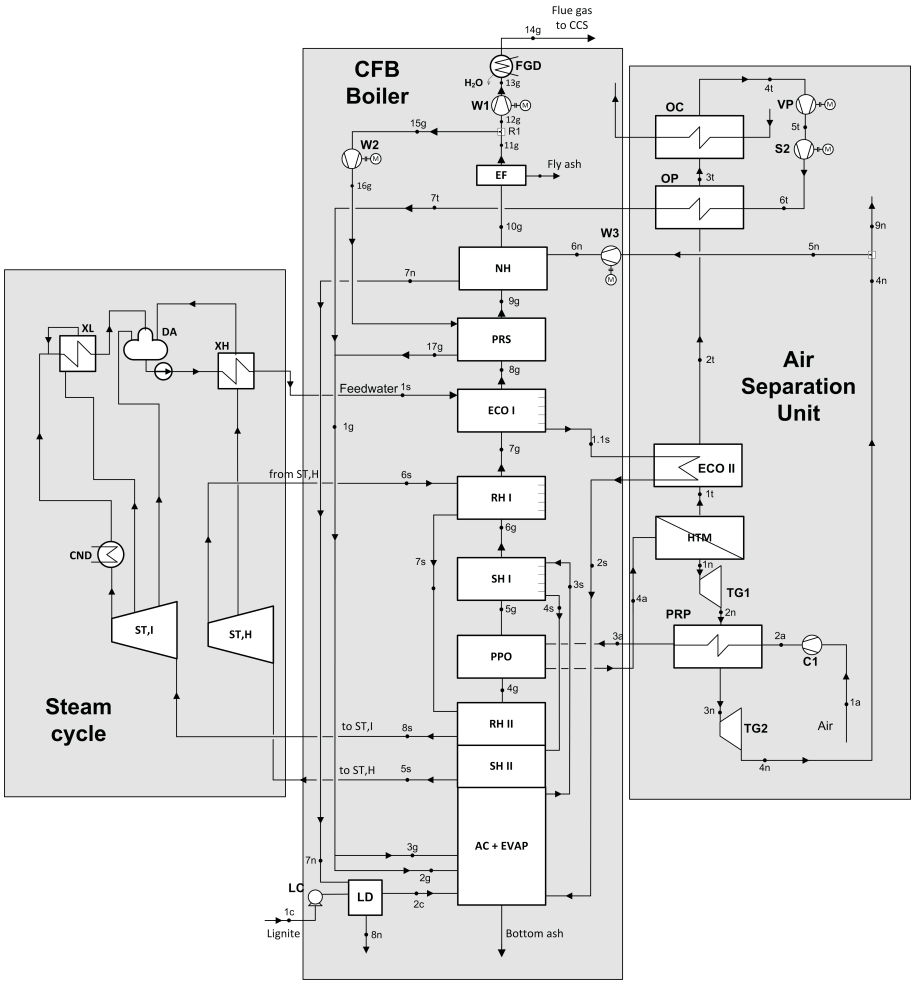

Figure 4. Scheme of CFB boiler integrated with air separation unit based on three-end type high temperature membrane

membrane were not assumed as well. Chosen assumptions for the calculations of an air separation unit are shown in Tab. 4.

Lignite dryer model was built as a simple heat exchanger in which the fuel stream is dried by the drying medium (a mixture of nitrogen and the oxygen derived from ASU). Drying medium is pre-heated in a heat exchanger placed in the path of exhaust gas within the convective pass of the CFB boiler. Chosen assumptions for a lignite dryer are shown in Tab. 5.

Table 4. Main assumptions for ASU installation.

Air pressure at the outlet of compressor	kPa	1400
Feed temperature	°C	850
Permeate pressure	kPa	425
Oxygen content in the permeate	%	100
Permeate temperature	°C	850
Retentate temperature	°C	850
Oxygen temperature at the inlet to the vacuum pump	°C	20
Air compressor isentropic efficiency		0.88
Expanders isentropic efficiency		0.90
Vacuum pump isentropic efficiency		0.88
Temperature difference at the hot end of oxygen heater PU	K	40

Table 5. Main assumptions for lignite dryer.

Lignite temperature at the inlet to the dryer	°C	15
Drying medium temperature at the outlet of the dryer	°C	130
Minimum temperature difference between lignite and drying medium	K	20
Temperature difference at the hot end of drying medium heater PA	K	30
Drying medium pressure at the outlet of the drying medium fan	kPa	108

The amount of heat that can be used to evaporate the moisture was determined from the formula

$$\dot{Q}_{vap} = \dot{Q}_{7n} - \dot{Q}_{8n} + \dot{I}_{1c} - \dot{I}_{2c} \, . \tag{10}$$

The mass flow of moisture evaporated in the drying process from the fuel is determined by the formula

$$\dot{m}_{H_2O_{vap}} = \frac{\dot{Q}_{vap}}{(r + c_s \cdot \Delta T)} \tag{11}$$

After evaporation of the moisture contained in the fuel the new lower heating value of the fuel must be determined:

$$W_{2c} = W_{1c} \left(\frac{1 - w_{2c}}{1 - w_{1c}} \right) + \left(\frac{w_{1c} - w_{2c}}{1 - w_{1c}} \right) r \, . \tag{12}$$

Once a new fuel calorific value is calculated boiler thermal efficiency could be determined from the formula:

$$\eta_{tk} = \frac{\dot{m}_{5s} \left(h_{5s} - h_{1s} \right) + \dot{m}_{8s} \left(h_{8sl} - h_{6s} \right)}{\dot{m}_{1c} W_{1c}} \, . \tag{13}$$

Evaluation of the effectiveness of the ASU installation are the auxiliaries of the installation defined as

$$\delta_{ASU} = \frac{N_{el,S1} + N_{el,VP} - N_{el,TG1} - N_{el,TG2}}{N_{el.g}} \,. \tag{14}$$

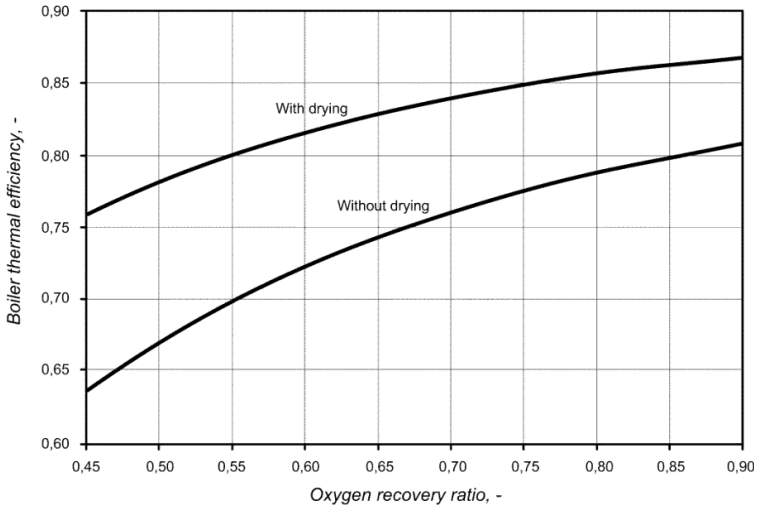

Figure 5. Boiler thermal efficiency as a function of oxygen recovery ratio in the membrane.

For the variant with fuel drying (Fig. 5), despite a higher the lower heating value (LHV) of fuel for low volumes of recovery of oxygen recovery ratios in the membrane, the boiler thermal efficiency increases with the oxygen recovery ratio up to the value of 86.8%. For the oxygen recovery ratio equal to 0.9 in case with lignite drying an increase in thermal efficiency of the boiler by six percentage points in comparison to the variant without drying was observed while for the oxygen recovery ratio at 0.45 increase in the thermal efficiency was equal to 12 p.p.

Although the gross power of the steam generator in the steam cycle is maintained at a constant level this case does not take into account the amount of power that can be generated in the generator of ASU installation. In the whole range of oxygen recovery ratio ASU installation auxiliaries are less than zero, which means that this installation will provide additional electricity to the system (Fig. 6).

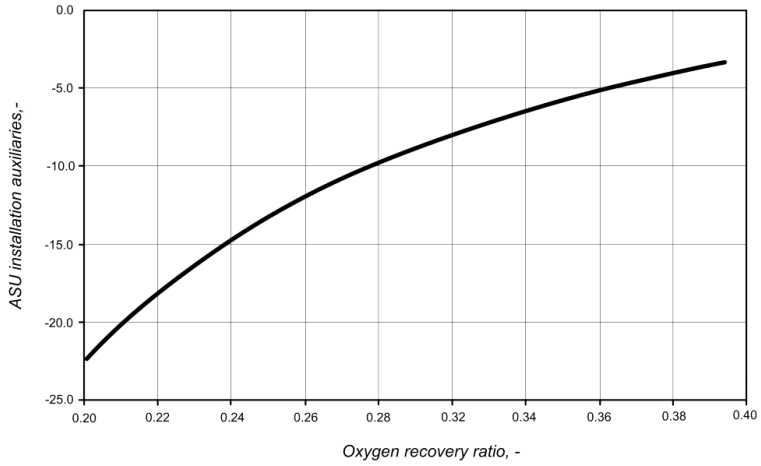

Figure 6. ASU installation auxiliaries as a function of oxygen recovery ratio in the membrane.

4 Summary

The increase in oxygen recovery ratio in the membrane results in an increase of thermal efficiency of the boiler. In case with fuel drying in a range of oxygen recovery ratio from 0.45 to 0.9 an increment in boiler thermal efficiency is higher than 11 p.p. The increase in thermal efficiency of the boiler in comparison to the case without dryer ranges from 12 p.p. for the recovery of oxygen equal to 0.45 to 6 p.p. for the recovery of oxygen equal to 0.9. Basing on the outcome results it can be concluded that the fuel drying in oxy type systems fed by lignite leads to a significant increase in the boiler thermal efficiency. Simultaneously, ASU installation auxiliaries are increasing from -52% to -4%, which means less amount of electric power generated in this installation. Surface of the membrane module from 76500 to 95000 m^2 also increases, which results in significant increment in investments costs of the ASU installation. In the future, the model must be completed with the CCS due to the significant impact on the efficiency of the system [11–14].

Acknowledgements The results presented in this paper were obtained from research work co-financed by the National Centre for Research and Development within a framework of Contract SP/E/2/66420/10 – Strategic Research Programme – Advanced Technologies for Energy Generation: Development of

a technology for oxy-combustion pulverized fuel and fluid boilers integrated with CO_2 capture.

Received in August 2012

References

[1] The technical report of step 6.1 in research topic: *Numerical simulations and systemic analysis of oxy – burning*, the research task 2 *Development of a technology for oxy-combustion pulverized-fuel and fluid boilers integrated with CO_2 capture in the strategic program of research and development*, Advanced Technologies for Energy Generation.

[2] Kotowicz J., Dryjańska A., Balicki A.: *Influence of the selected parameters for a CFB oxy boiler efficiency*. Rynek Energii 2(99), 2012, 120–126 (in Polish).

[3] Stadler H. it et al.: *Oxyfuel coal combustion by efficient integration of oxygen transport membranes*. International Journal of Greenhouse Gas Control **5**(2011), 7–15.

[4] Castillo R.: *Thermodynamic analysis of a hard coal oxyfuel power plant with high temperature three-end membrane for air separation*. Applied Energy **88**(2011), 1480–1493.

[5] Pfaff I., Kather A.: *Comparative thermodynamic analysis and integration issues of CCS steam power plants based on oxy-combustion with cryogenic or membrane based air separation*. Energy Procedia **1**(2009), 495–502.

[6] Chmielniak T.: *The role of various technologies in achieving emissions objectives in the perspective of the years up to 2050*. Rynek Energii, 1(92), 2011, 3–9 (in Polish).

[7] Skorek–Osikowska A., Bartela Ł.: *Model of a supercritical oxy-boiler – analysis of the selected parameters*. Rynek Energii, 5(90), 2010, 69–75 (in Polish).

[8] Kotowicz J., Bartela Ł.: *Optimization of the connection of membrane CCS installation with a supercritical coal-red power plant*. Energy **38**(2012), 118–127.

[9] Kotowicz J., Skorek-Osikowska A., Janusz - Szymańska K.: *Membrane separation of carbon dioxide in the integrated gasification combined cycle systems*. Archives of Thermodynamics **31**(2010), 3, 145–164.

[10] Janusz-Szymańska K., Kotowicz J.: *Analysis of CO_2 membrane separation process in the ultra supercritical coal fired power plant*. Rynek Energii **94**(2011), 3, 53–56 (in Polish).

[11] Kotowicz J., Janusz-Szymańska K.: *Influence of membrane CO_2 separation on the operating characteristics of a coal-fired power plant*. Chemical and Process Engineering **31**(2010), 4, 681–698.

[12] Kotowicz J., Janusz-Szymańska K.: *Influence of CO_2 separation on the efficiency of the supercritical coal fired power plant*. Rynek Energii **93**(2011), 2, 8–12 (in Polish).

[13] Kotowicz J., Janusz-Szymańska K.: *Selected methods to reduce energy consumption of carbon capture and storage installation in ultra-supercritical power plant*. Archives of Energetics, XLI(2011), 3-4, 97–110.

[14] Kotowicz J., Skorek-Osikowska A., Bartela Ł.: *Economic and environmental evaluation of selected advanced power generation technologies*. Proc. Institution of Mechanical Engineers, Part A: Journal of Power and Energy **225**(2011), 3, 221–232.

Analiza efektywności układu kotła cyrkulacyjnego typu oxy z membraną wysokotemperaturową typu *three-end* do separacji powietrza

S t r e s z c z e n i e

W artykule analizie poddano kocioł z cyrkulacyjnym złożem fluidalnym. Do spalania węgla brunatnego w kotle użyto tlenu wytworzonego w wysokotemperaturowej membranie typu *three-end*. Pokazano sposób określenia powierzchni membran oraz energochłonności procesu membranowej separacji powietrza. Sprawność termiczną kotła, energochłonność membranowej separacji powietrza i powierzchnię modułu membranowego wyznaczono w funkcji odzysku tlenu w membranie. Zaproponowano wykorzystanie azotu z instalacji separacji powietrza do suszenia węgla. Dla takiego wariantu również wwyznaczono charakterystyki układu. Stwierdzono, że przy wykorzystaniu azotu do suszenia sprawności termicznej kotła rośnie z 76% do 87%, przy wzroście stopnia odzysku tlenu od 0,45 do 0,9, i jest wyższa odpowiednio od 12% do 6% w porównaniu do układu bez suszenia. W zaproponowanym układzie separacji powietrza powierzchnia modułu membranowego zawiera się w przedziale 76,5–95,0 tys. m^2.